

approximation methods by which Eq. (7) can be derived.

<sup>5</sup>In statistical mechanics of classical fluids, Eq. (7) is also called the convolution hypernetted chain (CHNC) equation, with  $u(r) = -v(r)/k_B T$ .

<sup>6</sup>W. E. Massey and C. -W. Woo, Phys. Rev. **164**, 256 (1967).

<sup>7</sup>C. E. Campbell and E. Feenberg, Phys. Rev. **188**, 396 (1969).

<sup>8</sup>J. K. Percus and G. J. Yevick, Phys. Rev. **110**, 1

(1958); J. K. Percus, Phys. Rev. Letters **8**, 462 (1962).

<sup>9</sup>D. K. Lee, Phys. Rev. A **2**, 278 (1970).

<sup>10</sup>D. K. Lee and E. Feenberg, Phys. Rev. **137**, A731 (1965).

<sup>11</sup>D. K. Lee, Phys. Rev. **187**, 326 (1969).

<sup>12</sup>L. Verlet, Physica **30**, 95 (1964).

<sup>13</sup>A relation similar to (but simpler than) the PY II was considered for liquid He<sup>4</sup> by W. P. Francis, G. V. Chester, and L. Reatto, Phys. Rev. A **1**, 86 (1970).

## Resolution of the Hierarchy of Green's Functions for Fermions\*

Shigeji Fujita

Department of Physics and Astronomy, State University of New York, Buffalo, New York 14214

(Received 11 January 1971)

The rigorous evolution equations for the one-body Green's functions ( $g^>$ ,  $g^<$ ) describing a system of interacting fermions are not closed (an analog of the Bogoliubov-Born-Green-Kirkwood-Yvon hierarchy for many-body distribution functions). The analysis of these equations is made in terms of proper connected diagrams. It is established that in the bulk limit,  $N$  (particle number)  $\rightarrow \infty$ ,  $\Omega$  (volume)  $\rightarrow \infty$  while  $N/\Omega$  remains finite, these equations can rigorously be transformed into closed equations with respect to ( $g^>$ ,  $g^<$ ).

### I. INTRODUCTION

It has been known in classical-statistical mechanics that the rigorous evolution equations for reduced phase-space distribution functions describing an imperfect gas are coupled. These equations are often called the Bogoliubov-Born-Green-Kirkwood-Yvon (BBGKY) *hierarchy*.<sup>1</sup> In an earlier paper<sup>2</sup> the present author showed that the hierarchy equation of the lowest order can be transformed into a *closed* equation [Ref. 2, Eq. (2.26)] with respect to the one-body phase-space distribution function in the *bulk limit*:  $N$  (particle number)  $\rightarrow \infty$ ,  $\Omega$  (volume)  $\rightarrow \infty$  while  $N/\Omega$  (mean number density) remains finite. This is done using the analysis in terms of connected diagrams.<sup>3</sup> A restrictive feature of this analysis is that it is applicable to a system of distinguishable particles obeying the Boltzmann statistics, and not to a quantum statistical gas. This limitation can be overcome by working with double-time Green's functions ( $g^>$ ,  $g^<$ ) in place of the single-time one-body distribution function or density matrix.

In the present paper it is shown that the *hierarchy* equations of the lowest order, i. e., those involving one- and two-body Green's functions (2.6) describing an imperfect Fermi gas can be transformed into *closed* equations (4.15) with respect to ( $g^>$ ,  $g^<$ ) in the bulk limit. This is done in the following way: The hierarchy equation (2.6) contains an integral of the product of the pairwise potential  $v$  and the two-body Green's functions  $g_2^>$ , (2.7). This in-

tegral is analyzed in terms of *proper connected diagrams*<sup>3</sup> and is shown to be expressible in terms of one-body Green's functions ( $g^>$ ,  $g^<$ ) and given initial correlation matrices  $\chi$ . In the transformation no approximations other than those which can be justified in the bulk limit are used. The initial condition can be quite general; it may involve arbitrary correlation and also inhomogeneity, which are, in general, describable in terms of  $\chi$  matrices.

The closed equations (4.15) obtained are similar to the equations discussed by Kadanoff and Baym<sup>4</sup> [Ref. 4, Eqs. (8.27) and (8.28)]. These authors treated Green's functions ( $g^>$ ,  $g^<$ ) defined with the choice of the grand-canonical density operator for the initial condition at  $t = -\infty$ . While this can be argued as a useful choice, with such a particular choice one can no longer discuss the role of a general initial condition. For such discussion one obviously needs Green's functions with an arbitrary condition at a definite initial time rather than Green's functions with a specialized condition at an indefinite initial time. Equations (4.15) contain terms involving  $\Delta^>$ ,  $\Delta^<$  in (4.13), whose nature is distinct from that of any terms appearing in the Kadanoff-Baym equations. These extra terms necessarily involve  $\chi$  describing the initial correlation. Our closed equations (4.15) contain those terms which are most appropriately represented by an infinite set of proper connected diagrams, prescribed in a definite manner. The mathematical structure of the equations is such

that they allow us to discuss the stationary state of the system in a convenient way, which, however, will be discussed in separate publications.

The present theory proceeds along the line in which the hierarchy of classical-statistical many-body Green's functions was resolved in an earlier paper.<sup>5</sup> While the two theories have much in common, including the main objective and method, they significantly differ in the resulting closed equations (4.15), and in one of the key steps, i. e., the decomposition of a many-body density matrix into products of correlation matrices (3.10). Since these differences cannot be guessed simply but must be worked out, the detailed development will be presented here.

The analysis in terms of proper connected diagrams is useful in the practical calculation of transport coefficients. However, the demonstration of this aspect of the theory will be given in separate publications. The fact that proper connected diagrams are defined independently of any representation (momentum, position, or other) has a definite advantage when one deals with systems of nonuniform densities or with systems of charged particles subjected to electromagnetic fields.

In Sec. II the hierarchy equations for Green's functions are derived. In Sec. III, the integral of the product of the pairwise potential and the two-body Green's function is expanded, using the infinite-order perturbation theory and the correlation-matrix expansion of the initial many-body density matrix. Each term of the expansion is decomposed again into a sum of contractions, and the latter are represented by diagrams. After the diagram analysis, a set of closed evolution equations for  $g^>$  and  $g^<$  is obtained in Sec. IV. Throughout the text the units are chosen such that  $\hbar = 1$ .

## II. HIERARCHY EQUATIONS FOR GREEN'S FUNCTIONS

Let us consider a system of interacting fermions contained in a volume  $\Omega$ , characterized by the Hamiltonian  $H$ ,

$$\begin{aligned} H &\equiv \int d^3r \psi^\dagger(\vec{r}) h_0 \left( \vec{r}, -i \frac{\partial}{\partial \vec{r}}, t \right) \psi(\vec{r}) \\ &+ \frac{1}{2} \lambda \iint d^3r_1 d^3r_2 v(\vec{r}_1 - \vec{r}_2) \psi^\dagger(\vec{r}_1) \psi^\dagger(\vec{r}_2) \psi(\vec{r}_2) \psi(\vec{r}_1) \\ &\equiv H_0 + \lambda V, \end{aligned} \quad (2.1)$$

where  $h_0$  is a single-particle Hamiltonian which may contain the energy due to an electromagnetic field in addition to the kinetic energy and  $v$  is the pairwise potential with  $\lambda$  being the coupling constant. The field operators  $\psi$ ,  $\psi^\dagger$  satisfy the anti-commutation rules

$$\begin{aligned} [\psi(\vec{r}_1), \psi^\dagger(\vec{r}_2)]_* &\equiv \psi(\vec{r}_1) \psi^\dagger(\vec{r}_2) + \psi^\dagger(\vec{r}_2) \psi(\vec{r}_1) \\ &= \delta^{(3)}(\vec{r}_1 - \vec{r}_2), \end{aligned} \quad (2.2)$$

$$[\psi(\vec{r}_1), \psi(\vec{r}_2)]_* = [\psi^\dagger(\vec{r}_1), \psi^\dagger(\vec{r}_2)]_* = 0.$$

We now define partial Green's functions  $g^>$ ,  $g^<$  by

$$\begin{aligned} g^>(1, 2) &\equiv g^>(\vec{r}_1 t_1, \vec{r}_2 t_2) \\ &\equiv -i \text{Tr}[\rho \psi(1) \psi^\dagger(2)], \\ g^<(1, 2) &\equiv i \text{Tr}[\rho \psi^\dagger(2) \psi(1)], \end{aligned} \quad (2.3)$$

where  $\rho$  is a density operator to be specified at the initial time  $t=0$ ; the symbol Tr means the many-body trace;  $\psi(1)$  and  $\psi^\dagger(2)$  are annihilation and creation operators in the Heisenberg picture

$$\begin{aligned} \psi(1) &\equiv \psi(\vec{r}_1, t_1) \equiv U^\dagger(t_1) \psi(\vec{r}_1) U(t_1), \\ \psi^\dagger(2) &\equiv U^\dagger(t_2) \psi^\dagger(\vec{r}_2) U(t_2); \end{aligned} \quad (2.4)$$

and  $U(t)$  is the unitary evolution operator satisfying

$$i \frac{\partial}{\partial t} U(t) = H(t) U(t), \quad U(0) = 1. \quad (2.5)$$

Differentiating  $g^<(1, 2)$  with respect to  $t_1$ , one obtains

$$\begin{aligned} i \frac{\partial}{\partial t_1} g^<(1, 2) &= \frac{i}{\Omega} \text{Tr}[\rho \psi^\dagger(2) U^\dagger(t_1) [H(t) \psi(\vec{r}_1) - \psi(\vec{r}_1) H(t)] U(t_1)] \\ &= h_0 \left( \vec{r}_1, -i \frac{\partial}{\partial \vec{r}_1}, t_1 \right) g^<(1, 2) \\ &+ \lambda \int d^3r_3 v(\vec{r}_3 - \vec{r}_1) g_2^<(\vec{r}_1 t_1, \vec{r}_3 t_1, \vec{r}_2 t_2, \vec{r}_3 t_1), \end{aligned} \quad (2.6)$$

where  $g_2^<$  is the two-body Green's function defined by

$$g_2^<(13, 24) \equiv i^2 \text{Tr}[\rho \psi^\dagger(2) \psi^\dagger(4) \psi(3) \psi(1)]. \quad (2.7)$$

We see in (2.6) that the exact behavior of the evolution of  $g^<$  is governed by the two-body Green's function  $g_2^<$ . In fact, Eq. (2.6) is one of the hierarchy equations analogous to the BBGKY hierarchy found for the classical many-body distribution functions. Since Eq. (2.6) contains two unknowns,  $g^<$  and  $g_2^<$ , one cannot contemplate solving it in the present form. This same situation holds for other evolution equations for  $g^>$  and  $g^<$  which are generated by differentiation with respect to  $t_1$  and  $t_2$ .

## III. DIAGRAM REPRESENTATION

In Sec. II, we have seen that the rigorous evolution of  $g^<$  is ruled by the hierarchy equation (2.6).

The origin of this complexity lies in the particle correlation generated by the pairwise interaction. The single-particle Hamiltonian due to a possible electromagnetic field does not contribute to this complexity. Since we are primarily interested in resolving the hierarchy in the present theoretical development, we shall exclude external fields from our consideration. We may then assume that

the single-particle Hamiltonian  $h_0$  is a function of the momentum only, and is independent of time:

$$h_0(\vec{p}) \equiv h_0 \left( -i \frac{\partial}{\partial \vec{r}} \right). \quad (3.1)$$

The second term of the third member of (2.6) can be written as

$$\begin{aligned} & i\lambda \int d^3r_3 v(\vec{r}_1 - \vec{r}_3) \text{Tr}[\rho \psi^\dagger(2) U^\dagger(t_1) \psi^\dagger(\vec{r}_3) \psi(\vec{r}_3) \psi(\vec{r}_1) U(t_1)] \\ & = i\lambda \int d^3r_3 v(\vec{r}_1 - \vec{r}_3) \text{Tr}[\rho U_D^\dagger(t_2) \psi_2^\dagger(t_2) U_D(t_2, t_1) \psi_3^\dagger(t_1) \psi_3(t_1) \psi_1(t_1) U_D(t_1)], \end{aligned} \quad (3.2)$$

where

$$U_D(t) \equiv e^{itH_0} U(t), \quad (3.3)$$

$$U_D(t_2, t_1) \equiv e^{it_2 H_0} U(t_2) U^\dagger(t_1) e^{-it_1 H_0},$$

$$\psi_j(t) \equiv \psi_{\vec{r}_j}(t) \equiv e^{itH_0} \psi(\vec{r}_j) e^{-itH_0}, \quad (3.4)$$

$$\psi_j^\dagger(t) \equiv e^{itH_0} \psi^\dagger(\vec{r}_j) e^{-itH_0}.$$

The operators  $U_D^\dagger$ ,  $U_D$ , and  $U$  are functions of  $\lambda$ , and can be expanded in powers of  $\lambda$ :

$$\begin{aligned} U_D(t) &= 1 + \sum_1^\infty (-i\lambda)^k \int_0^t d\tau_1 \int_0^{\tau_1} d\tau_2 \cdots \\ & \quad \times \int_0^{\tau_{k-1}} d\tau_k V(\tau_1) V(\tau_2) \cdots V(\tau_k), \end{aligned} \quad (3.5)$$

$$U_D(t_2, t_1) = 1 + \sum_1^\infty (-i\lambda)^k \int_{t_1}^{t_2} d\tau_1 \int_{t_1}^{\tau_1} d\tau_2 \cdots$$

$$\times \int_{t_1}^{\tau_{k-1}} d\tau_k V(\tau_1) V(\tau_2) \cdots V(\tau_k),$$

$$V(\tau) \equiv e^{i\tau H_0} V e^{-i\tau H_0}$$

$$= \frac{1}{2} \int \int d^3r_1 d^3r_2 v(\vec{r}_1 - \vec{r}_2) \psi_1^\dagger(\tau) \psi_2^\dagger(\tau) \psi_2(\tau) \psi_1(\tau). \quad (3.6)$$

A many-body density operator  $\rho$  to be specified at the initial time contains all information about the inhomogeneity and particle correlation of the system. The latter can equivalently be obtained from the reduced density matrices  $\rho_n$  defined by

$$\langle \alpha_r | \rho_1 | \alpha_s \rangle \equiv \text{Tr}(\rho a_s^\dagger a_r), \quad (3.7)$$

$$\langle \alpha_r \alpha_t | \rho_2 | \alpha_s \alpha_u \rangle \equiv \text{Tr}(\rho a_s^\dagger a_u^\dagger a_t a_r),$$

...

where  $|\alpha_s\rangle$ ,  $\langle \alpha_r|$  are ket and bra vectors characterized by the states  $\alpha_s$ ,  $\alpha_r$ ;  $a_s^\dagger$ ,  $a_r$  are creation

and annihilation operators for the states  $\alpha_s$ ,  $\alpha_r$ . They satisfy the usual anticommutation relations similar to (2.2):

$$\begin{aligned} [a_r, a_s^\dagger]_\pm &= \delta_{r,s}, \\ [a_s, a_r]_\pm &= [a_s^\dagger, a_r^\dagger]_\pm = 0, \end{aligned} \quad (3.8)$$

where  $\delta_{r,s}$  is Kronecker's  $\delta$  for the case of discrete states and the Dirac  $\delta$  function for that of continuous states. (These states may be position states, and in that case the creation and annihilation operators are denoted by the letters  $\psi^\dagger$ ,  $\psi$ .)

From the definition (3.7) and the anticommutation relations (3.8), the two-body density-matrix elements satisfy

$$\langle \alpha_1 \alpha_2 | \rho_2 | \alpha_3 \alpha_4 \rangle \equiv \rho_2(12, 34) = -\rho_2(21, 34). \quad (3.9)$$

More generally,

$$\begin{aligned} P_k \rho_k(1 2 \cdots k, (k+1) \cdots (2k)) \\ = \delta_{P_k} \rho_k(1 2 \cdots k, (k+1) \cdots (2k)), \end{aligned} \quad (3.9')$$

where  $P_k$  is an arbitrary permutation for the set of numerals  $1, 2, \dots, k$ , and  $\delta_P$  is the parity sign; i. e., it is either 1 or  $-1$  according to whether  $P$  is an even or odd permutation.

Let us now define the *pair-correlation matrix*  $\chi_2$  by

$$\begin{aligned} \rho_2(12, 34) \\ = \rho_1(1, 3) \rho_1(2, 4) - \rho_1(1, 4) \rho_1(2, 3) + \chi_2(12, 34). \end{aligned} \quad (3.10)$$

By applying the exchange operator (1, 2) and using (3.9), one obtains

$$\chi_2(12, 34) = -\chi_2(21, 34), \quad (3.11)$$

which means that  $\chi_2$  has the same antisymmetry as  $\rho_2$ .

From the definitions of  $\rho_1$ ,  $\rho_2$ , in (3.7),

$$\begin{aligned} \text{Lim} \frac{1}{\Omega} \int d(1) \rho_1(1, 1) &= \text{Lim} \frac{1}{\Omega} \text{Tr} \left( \rho \int d(1) a_1^\dagger a_1 \right) \\ &= \text{Lim} \frac{N}{\Omega} = n, \end{aligned} \quad (3.12)$$

$$\begin{aligned} \text{Lim} \frac{1}{\Omega} \int d(2) \rho_2(12, 23) &= \text{Lim} \frac{1}{\Omega} \\ &\times \text{Tr} \left[ \rho a_3^\dagger \left( \int d(2) a_2^\dagger a_2 \right) a_1 \right] \end{aligned}$$

where the symbol Lim means the bulk limit. Using these, we obtain from (3.10)

$$\begin{aligned} \text{Lim} (1/\Omega) \int d(2) \chi_2(12, 32) \\ &= \text{Lim} (1/\Omega) \int d(2) [\rho_2(12, 32) - \rho_1(1, 3) \rho_1(2, 2) \\ &\quad + \rho_1(1, 2) \rho_1(2, 3)] \\ &= \text{Lim} (1/\Omega) \langle \alpha_1 | \rho_1^2 | \alpha_3 \rangle. \end{aligned}$$

Since  $\langle \alpha_1 | \rho_1^2 | \alpha_3 \rangle$  can safely be assumed to be finite, we obtain

$$\text{Lim} (1/\Omega) \int d(2) \chi_2(12, 32) = 0. \quad (3.13)$$

This is an important property of the pair-correlation matrix defined by (3.10) (see below).

We now wish to define many-body correlation matrices  $\chi_k$ ,  $k \geq 2$  such that they should have properties which are the generalizations of (3.11) and (3.13). The results are

$$\begin{aligned} \rho_3(123, 456) &= \sum_{P_3} \delta_{P_3} P_3 [\rho_1(1, 4) \rho_1(2, 5) \rho_1(3, 6) \\ &\quad + \rho_1(1, 4) \chi_2(23, 56) + \rho_1(2, 5) \chi_2(13, 46) \\ &\quad + \rho_1(3, 6) \chi_2(12, 45)] + \chi_3(123, 456), \text{ etc.}, \end{aligned} \quad (3.10')$$

$$\begin{aligned} P_k \chi_k(12 \dots k, (k+1) \dots (2k)) \\ &= \delta_{P_k} \chi_k(12 \dots k, (k+1) \dots (2k)), \end{aligned} \quad (3.11')$$

$$\text{Lim} (1/\Omega) \int d(1) \chi_k(12 \dots k, 1(k+2) \dots (2k)) = 0. \quad (3.13')$$

It is noted that the antisymmetric products are taken in (3.10) and (3.10') in contrast to the classical case. It is also noted that this decomposition of reduced density matrices into products of correlation matrices can rigorously be defined only in the bulk limit, and it is done independently on any representation (position, momentum, or other representation).

It is clear that we can specify the initial condi-

tion by giving  $\rho_1, \chi_2, \dots$  instead of a single many-body  $\rho$ . In fact, this specification is obviously more realistic.

We now propose to replace the  $N$ -body density matrix  $\rho$  by the reduced  $N$ -body density matrix  $\rho_N$  defined with an ensemble of still larger systems, and decompose the latter  $\rho_N$  by the procedure (3.10')

$$\rho_N = \mathfrak{A}(\Pi \rho_1 + \chi_2 \Pi \rho_1 + \dots) + \chi_N, \quad (3.14)$$

where the symbol  $\mathfrak{A}$  means the antisymmetrization of the products.

With the aid of (3.5) and (3.14), we can expand the last member of (3.2). Each component of this expansion can be decomposed into the sum of *contractions*, i. e., products of contracted pairs (see below). This decomposition is discussed in Ref. 3, pp. 87–89, and will not be reproduced here. Essentially, this is based on the contraction theorem<sup>6</sup> applied for the diagonal element of any product of fermion operators. For any four fermion operators  $U, V, W$ , and  $X$ , the theorem reads

$$\begin{aligned} \langle n | U V W X | n \rangle \\ &= U^* V^* W^* X^* + U^* V^* W^* X^* + U^* V^* W^* X^*, \end{aligned} \quad (3.15)$$

$$\begin{aligned} U^* V^* W^* X^* &\equiv \delta_P (U^* W^*) (V^* X^*) \\ &= - (U^* W^*) (V^* X^*), \end{aligned} \quad (3.16)$$

where *contracted pairs* defined by

$$U^* V^* \equiv \langle n | U V | n \rangle \quad (3.17)$$

are denoted by dots and double dots, and  $\delta_P = \pm 1$  is the parity of permutation  $P$  which transposes the ordered contraction on one member of equality into that on another member [see (3.16)];  $|n\rangle, \langle n|$  are normalized ket and bra for many-fermion states.

Now each contraction can be conveniently represented by a diagram.

Draw a horizontal boundary line. The operator  $\psi_2^\dagger(t_2)$  is denoted by a point above the boundary at  $t=t_2$  at which a particle line is to start, and  $\psi_2^\dagger(t_1) \psi_3(t_1) \psi_1(t_1)$  by a point at  $t=t_1$ , at which two particle lines are to arrive and a particle line is to start. The time is measured from right to left with the right end corresponding to  $t=0$ . All the interactions  $V(\tau)$  arising from the three ( $U_D^t, U_D', U_D$ ) can be ordered according to their time arguments  $\tau$ : Those  $V(\tau)$  from  $U_D^t(t_2)$  are represented by vertices below the boundary line, those  $V(\tau)$  from  $U_D(t_1)$  by vertices above the boundary, and those  $V(\tau)$  from  $U_D'(t_1, t_2)$  are represented by vertices above or below the boundary according to whether

$t_2 > t_1$  or  $t_2 < t_1$ . Each of these vertices will have two particle lines arriving and two particle lines leaving, which arises from the fact that  $V(\tau)$  contains two annihilation and two creation operators. The correlation matrices  $\chi_l$ ,  $l \geq 2$ , are represented by a point below the boundary at  $t=0$ , where  $l$  particle lines are to arrive and also  $l$  particle lines are to leave. To avoid complexity we do not represent  $\rho_1$  in the diagram. This could have been done by using a point below the boundary at  $t=0$  where one particle line should arrive and one particle line should leave.

A diagram is completed by drawing particle lines from a point to itself or to another. A diagram so completed, in fact, corresponds to an in general nonvanishing contracted component of the trace in (3.2). Other conceivable diagrams not in accordance with the above prescription correspond to either trivially vanishing contractions or none at all.

#### IV. DIAGRAM ANALYSIS: CLOSED EQUATIONS FOR $(g^>, g^<)$

A diagram is said to be *connected* if any two points on it can be reached from one to the other without leaving it. Otherwise, the diagram will be called *disconnected*. For example, Fig. 1(a) is connected while Fig. 1(b) is disconnected. All the disconnected diagrams do not contribute to (3.2) effectively although a particular diagram may contribute a finite amount. This can be proved with the aid of the following two theorems.

*Theorem I.* Any diagram containing an  $M$ -type potential vertex has a counterpart such that the pair so found yield mutually cancelling contributions.

A *potential vertex of the  $M$  type* is a vertex which has all the incoming and outgoing lines on the right. For example, Figs. 1(b) and 1(c) have such vertices  $M$  and, in fact, form the pair which are recognized by the location of the  $M$  vertices above and below the boundary line and which have mutually cancelling contributions. The proof of this theo-

rem essentially rests on the fact that the potential vertices above and below the boundary, arising from  $U_D(t)$  and  $U_D^\dagger(t)$ , have different signs as seen from (3.5). It is stressed that the recognition of the mutually cancelling pair is particularly easy in our diagram representation. This theorem holds for a finite system, and it is valid irrespective of whether the system obeys Maxwell-Boltzmann, Bose-Einstein, or Fermi-Dirac statistics.

*Theorem II.* Any diagram containing a correlation vertex with one or more particle loops contributes nothing.

Figure 1(d) contains a correlation vertex with two loops and yields vanishing contribution. This arises from the fact that such a correlation vertex contributes a vanishing factor of the form (3.13'). This theorem is strictly valid in the bulk limit.

Any disconnected diagram has either a  $M$ -type potential vertex or a correlation vertex with loops or both as seen in Figs. 1(b)–1(d) and therefore does not effectively contribute.

The power of these two theorems is not limited to the elimination of the disconnected diagrams. In fact it allows us to disregard a large number of connected diagrams. For example, Figs. 2(a) and 2(b) are connected diagrams but these diagrams contain a  $M$ -type potential vertex and correlation vertex with a loop, respectively, and therefore need not be considered in the further diagram analysis.

A connected diagram may or may not consist of two parts which can be separated out by cutting a pair of particle lines. In the first case we shall say that it is an *improper* diagram; and in the latter case it is *proper*. For example, Fig. 3(a) is proper and Fig. 3(b) improper. A part which is suspended by such a pair of lines will be called a *self-energy part*, following the terminology used in the quantum field theory. We shall further say that we *reduce* an improper diagram into a simpler diagram when we suppress its self-energy parts. If we repeatedly make such reduction for an arbitrary improper diagram, we shall finally come

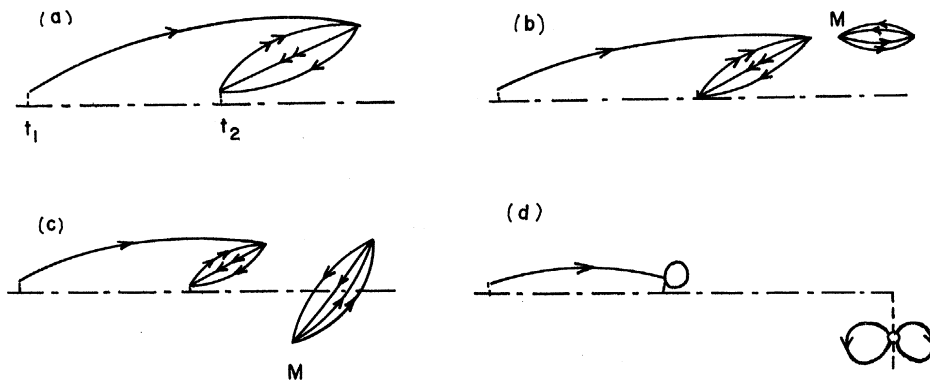


FIG. 1. (a) is a connected diagram, and all others are disconnected diagrams. (b) and (c) have  $M$ -type potential vertices and mutually cancelling contributions. (d) has a correlation vertex with two loops and contributes nothing.

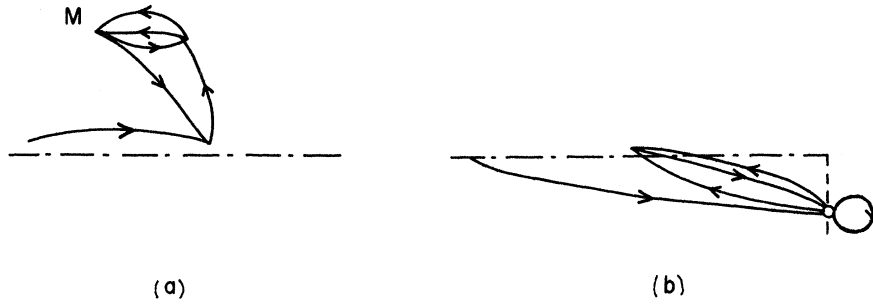


FIG. 2. (a) is a connected diagram but effectively contributes nothing because it contains an  $M$ -type potential vertex. (b) contributes nothing because it contains a correlation vertex with a loop.

down to a proper diagram. For example, Fig. 3(b) is uniquely reducible to Fig. 3(a). Conversely, one can generate improper diagrams from a proper diagram by *dressing* its particle lines with self-energy parts. It is noted that this dressing must be made to the right because otherwise it would necessarily generate  $M$ -type potential vertices and would contribute nothing. In view of this diagram analysis one can reclassify the infinite set of connected diagrams by first enumerating proper connected diagrams and then generating improper diagrams by dressing.

It is easily verified that in any proper diagram the particle line starting from the point at  $t=t_2$  must end either (i) at the point at  $t=t_1$ , (ii) at a potential vertex at  $t=t_3$  which may arise from the three operators ( $U_D, U'_D, U''_D$ ), or (iii) at a correlation vertex at  $t=0$  which arises from the initial density operator  $\rho$ . Examples of the three alternatives are, respectively, those diagrams in Figs. 4(a), 3(a), and 4(b).

In the first alternative (i) the contribution of the only proper diagram in Fig. 4(a) is given by

$$U_0(1)g_0^<(1, 2), \quad (4.1)$$

$$U_0(1) \equiv -i\lambda \int d^3r_3 v(\vec{r}_1 - \vec{r}_3)g_0^<(\vec{r}_3, t_1, \vec{r}_3, t_1), \quad (4.2)$$

where the double space-time functions  $g_0^<$  (and  $g_0^>$ ) are defined by

$$\begin{aligned} g_0^<(1, 2) &\equiv i \text{Tr}[\rho \psi_2^\dagger(t_1) \psi_1(t_1)], \\ g_0^>(1, 2) &\equiv -i \text{Tr}[\rho \psi_1(t_2) \psi_2(t_2)] \end{aligned} \quad (4.3)$$

and will be referred to as partial Green's functions corresponding to free particles or simply as *free-particle* Green's functions.

In general the mathematical expression can be readily read off from a given diagram: A particle line running from 2 to 1 contributes either  $g_0^>(1, 2)$  or  $g_0^<(1, 2)$  according to whether it proceeds in the *positive sense*; i. e., from left to right above the boundary line, from right to left below or downward when crossing the boundary, or in the non-positive sense; a particle loop contributes a  $g_0^<$ ; a potential vertex contributes a factor  $+i\lambda v$  or  $-i\lambda v$  according to whether it is above or below the boundary line; and a correlation vertex with  $l$  pairs of incoming and outgoing lines contributes a factor  $\chi_l$ . The resulting expression is to be integrated with respect to all time variables without changing the time order and also to be integrated with respect to all space variables.

It is now asserted that in the bulk limit the total contribution of this proper diagram, and all improper diagrams which can be generated from it, can be accounted for by

$$U(1)g^<(1, 2), \quad (4.4)$$

$$U(1) \equiv -i\lambda \int d^3r_3 v(\vec{r}_1 - \vec{r}_3)g^<(\vec{r}_3, t_1, \vec{r}_3, t_1), \quad (4.5)$$

which may be obtained from (4.1) and (4.2) by omitting the subscripts 0. This can be proved in a standard way in which two infinite sets are compared: Choose an arbitrary improper diagram and look for, and verify, the corresponding diagram of the same order in  $\lambda$  within the diagram expansion of (4.4). Conversely, find the correspondence by starting with an arbitrary diagram representing the expansion of (4.4). This correspondence can be rigorously established in the bulk limit. In this identification it is important to remember that the dressing of a free-particle line should be done

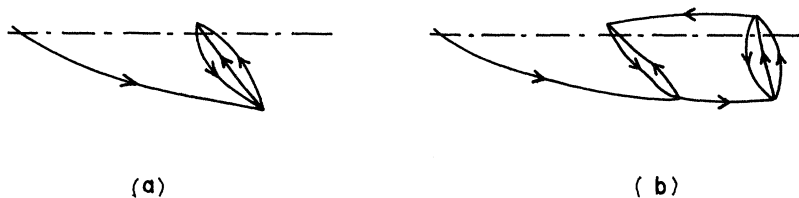


FIG. 3. Improper diagram (b) is uniquely reducible to the proper diagram (a).

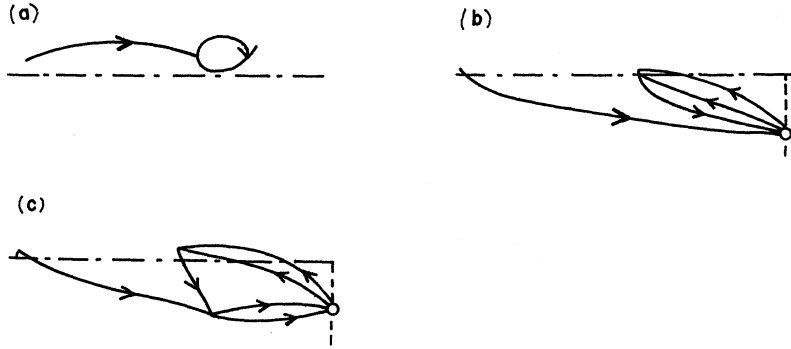


FIG. 4. (a) contributes the expression (4.1). (b) is a member of the diagrams contributing to (4.12), while (c) is a member of diagrams contributing to (4.10).

always to the right, i. e., in the direction of the decreasing time since the dressing made otherwise would introduce necessarily an  $M$ -type potential vertex as seen in Fig. 2(a), and therefore would give no effective contribution.

This way of obtaining the contribution of the proper diagram and the improper diagrams associated with it, is not restricted to this particular diagram Fig. 4(a). In fact, it is valid in general.

The class of proper diagrams corresponding to the second alternative (ii) can be further divided into two classes, those diagrams whose self-energy parts with the vertices at  $t=t_1$  and  $t_3$  consist of potential vertices plus particle lines running between them such as Fig. 3(a), and those diagrams whose self-energy parts are composed of potential vertices and correlation vertices plus particle lines running between them such as Fig. 4(c). Corresponding to this subdivision, the contribution of the self-energy parts can be written as the sum of the two parts:

$$\begin{aligned}\Sigma^>(1, 3) &\equiv \Sigma_1^>(1, 3) + \Sigma_2^>(1, 3; \chi), \\ \Sigma^<(1, 3) &\equiv \Sigma_1^<(1, 3) + \Sigma_2^<(1, 3; \chi),\end{aligned}\quad (4.6)$$

$$\begin{aligned}\Sigma^>(1, 3) &\equiv -i\lambda^2 \int \int d^3r_4 d^3r_5 \{v(\vec{r}_1 - \vec{r}_4)v(\vec{r}_3 - \vec{r}_5) \\ &\times \text{Tr}[\rho\psi^\dagger(\vec{r}_4, t_1)\psi(\vec{r}_4, t_1)\psi(\vec{r}_1, t_1) \\ &\times \psi^\dagger(\vec{r}_3, t_3)\psi^\dagger(\vec{r}_5, t_3)\psi(\vec{r}_5, t_3)]\}_\sigma, \\ \Sigma^<(1, 3) &\equiv -i \int \int d^3r_4 d^3r_5 \{v(\vec{r}_1 - \vec{r}_4)v(\vec{r}_5 - \vec{r}_3) \\ &\times \text{Tr}[\rho\psi^\dagger(\vec{r}_3, t_3)\psi^\dagger(\vec{r}_5, t_3)\psi(\vec{r}_5, t_3) \\ &\times \psi^\dagger(\vec{r}_4, t_1)\psi(\vec{r}_4, t_1)\psi(\vec{r}_1, t_1)]\}_\sigma,\end{aligned}\quad (4.7)$$

where the subscript  $\sigma$  means that contribution corresponding to the whole set of proper self-energy parts and the subscripts 1 and 2 denote the two subdivisions described above. From the characteristics of the diagrams, it is verified that the self-energy parts  $\Sigma_1^>$  and  $\Sigma_1^<$  can be described in

terms of  $g^>$  and  $g^<$  only while  $\Sigma_2^>$  and  $\Sigma_2^<$  contain the initial correlation operators  $\chi$  by definition. For example, the proper self-energy part appearing in Fig. 3(a) contributes

$$\begin{aligned}\lambda^2 \int \dots \int d^3r_4 d^3r_5 v(\vec{r}_1 - \vec{r}_4)v(\vec{r}_3 - \vec{r}_5) \\ \times [g^<(\vec{r}_1 t_1, \vec{r}_3 t_3)g^<(\vec{r}_4 t_1, \vec{r}_5 t_3)g^>(\vec{r}_5 t_3, \vec{r}_4 t_1) \\ - g^<(\vec{r}_1 t_1, \vec{r}_5 t_3)g^<(\vec{r}_4 t_1, \vec{r}_3 t_3)g^>(\vec{r}_5 t_3, \vec{r}_4 t_1)],\end{aligned}\quad (4.8)$$

while the self-energy part appearing in Fig. 4(c) yields

$$\begin{aligned}\lambda^2 \int \dots \int \prod_4^9 d^3r_j v(\vec{r}_1 - \vec{r}_9)v(\vec{r}_3 - \vec{r}_4) \\ \times g^<(\vec{r}_1 t_1, \vec{r}_7 0)g^<(\vec{r}_5 t_1, \vec{r}_9 0)g^>(\vec{r}_5 0, \vec{r}_3 t_3) \\ \times g^>(\vec{r}_6 0, \vec{r}_4 t_3)g^>(\vec{r}_4 t_3, \vec{r}_1 t_1)\chi_2(\vec{r}_7 \vec{r}_8, \vec{r}_5 \vec{r}_6).\end{aligned}\quad (4.9)$$

Clearly, the potential vertex at  $t=t_3$  must originate in one of the three  $U_D$ ,  $U'_D$ , and  $U_D^\dagger$ . Corresponding to these three cases the contribution of the diagrams can be written as the sum of three distinct integrals

$$\begin{aligned}\int_0^{t_1} dt_3 \int d^3r_3 \Sigma^>(1, 3)g^<(3, 2) \\ + \int_{t_1}^{t_2} dt_3 \int d^3r_3 \Sigma^<(1, 3)g^<(3, 2) \\ - \int_0^{t_2} dt_3 \int d^3r_3 \Sigma^<(1, 3)g^>(3, 2).\end{aligned}\quad (4.10)$$

Here the difference between the classical- and quantum-statistical cases becomes particularly explicit. If the particle line starting from the vertex at  $t=t_2$  ends at a potential vertex arising from  $U'_D$ , it cannot proceed to the vertex at  $t=t_1$  without violating the restriction of the Boltzmann statistics that every particle line forming a loop

always should proceed in the positive sense.<sup>5</sup>  
Therefore, the middle term in (4.10), i. e.,

$$\int_{t_1}^{t_2} dt_3 \int d^3r_3 \Sigma^{\langle}(1, 3) g^{\langle}(3, 2) \quad (4.11)$$

should have been discarded completely in the Boltzmann-statistical case.

In the third alternative (iii), the contribution of such proper diagrams and their associated diagrams contain initial correlation matrices  $\chi$  and can be expressed in terms of  $g^{\rangle}$ ,  $g^{\langle}$ , and  $\chi$ . We may write this contribution in the form

$$\int d^3r_3 \Delta^{\langle}(1, \vec{r}_3 0; \chi) g^{\rangle}(\vec{r}_3 0, 2), \quad (4.12)$$

where the *destruction parts* ( $\Delta^{\rangle}$ ,  $\Delta^{\langle}$ ) may be generally written as

$$\Delta^{\rangle}(\vec{r}_3 0, 1; \chi) \equiv -\lambda \int d^3r_4 \{v(\vec{r}_1 - \vec{r}_4) \times \text{Tr}[\rho \psi^{\dagger}(1) \psi^{\dagger}(\vec{r}_4 t_1) \psi(\vec{r}_4 t_1) \psi(\vec{r}_3 0)]\}_{\sigma},$$

$$\Delta^{\langle}(1, \vec{r}_3 0; \chi) \equiv -\lambda \int d^3r_4 \{v(\vec{r}_1 - \vec{r}_4) \times \text{Tr}[\rho \psi^{\dagger}(\vec{r}_3 0) \psi^{\dagger}(\vec{r}_4, t_1) \psi(\vec{r}_4, t_1) \psi(1)]\}_{\sigma}. \quad (4.13)$$

In practice however it is easier to directly write down the contribution from the diagrams. For example, the destruction part appearing in Fig. 4(b) can be written out as

$$i\lambda \int \dots \int d^3r_4 d^3r_5 d^3r_6 d^3r_7 v(\vec{r}_1 - \vec{r}_4) g^{\langle}(1, \vec{r}_7 0) \times g^{\langle}(\vec{r}_4 t_1, \vec{r}_6 0) g^{\rangle}(\vec{r}_5 0, \vec{r}_4 t_1) \times \chi_2(\vec{r}_7 \vec{r}_6, \vec{r}_3 \vec{r}_5). \quad (4.14)$$

In summary, after the analysis in terms of proper connected diagrams we are able to transform the hierarchy equation (2.6) into

$$\left[ i \frac{\partial}{\partial t_1} - h_0 \left( -i \frac{\partial}{\partial \vec{r}_1} \right) - U(1) \right] g^{\langle}(1, 2) = \int_0^{t_1} dt_3 \int d^3r_3 \Sigma^{\rangle}(1, 3) g^{\langle}(3, 2) + \int_{t_1}^{t_2} dt_3 \int d^3r_3 \Sigma^{\langle}(1, 3) g^{\langle}(3, 2) - \int_0^{t_2} dt_3 \int d^3r_3 \Sigma^{\langle}(1, 3) g^{\rangle}(3, 2) - \int d^3r_3 \Delta^{\langle}(1, \vec{r}_3 0; \chi) g^{\rangle}(\vec{r}_3 0, 2). \quad (4.15a)$$

This is one of the *corrected* Kadanoff-Baym equations describing the evolution of partial Green's functions. The other three equations, all arising from the  $t_1$  and  $t_2$  derivatives of  $g^{\rangle}(1, 2)$  and  $g^{\langle}(1, 2)$ , can be analyzed and written out in a similar manner:

$$\left[ -i \frac{\partial}{\partial t_2} - h_0 \left( -i \frac{\partial}{\partial \vec{r}_2} \right) - U(2) \right] g^{\langle}(1, 2) = \int_0^{t_1} dt_3 \int d^3r_3 g^{\rangle}(1, 3) \Sigma^{\langle}(3, 2) + \int_{t_1}^{t_2} dt_3 \int d^3r_3 g^{\langle}(1, 3) \Sigma^{\langle}(3, 2) - \int_0^{t_2} dt_3 \int d^3r_3 g^{\langle}(1, 3) \Sigma^{\rangle}(3, 2) - \int d^3r_3 g^{\langle}(1, \vec{r}_3 0) \Delta^{\rangle}(\vec{r}_3 0, 2; \chi), \quad (4.15b)$$

$$\left[ i \frac{\partial}{\partial t_1} - h_0 \left( -i \frac{\partial}{\partial \vec{r}_1} \right) - U(1) \right] g^{\rangle}(1, 2) = \int_0^{t_2} dt_3 \int d^3r_3 \Sigma^{\rangle}(1, 3) g^{\langle}(3, 2) + \int_{t_2}^{t_1} dt_3 \int d^3r_3 \Sigma^{\rangle}(1, 3) g^{\rangle}(3, 2) - \int_0^{t_1} dt_3 \int d^3r_3 \Sigma^{\langle}(1, 3) g^{\rangle}(3, 2) - \int d^3r_3 \Delta^{\langle}(1, \vec{r}_3 0; \chi) g^{\rangle}(\vec{r}_3 0, 2), \quad (4.15c)$$

$$\left[ -i \frac{\partial}{\partial t_2} - h_0 \left( -i \frac{\partial}{\partial \vec{r}_2} \right) - U(2) \right] g^{\rangle}(1, 2) = \int_0^{t_2} dt_3 \int d^3r_3 g^{\rangle}(1, 3) \Sigma^{\langle}(3, 2) + \int_{t_2}^{t_1} dt_3 \int d^3r_3 g^{\rangle}(1, 3) \Sigma^{\rangle}(3, 2) - \int_0^{t_1} dt_3 \int d^3r_3 g^{\langle}(1, 3) \Sigma^{\rangle}(3, 2) - \int d^3r_3 g^{\langle}(1, \vec{r}_3 0) \Delta^{\rangle}(\vec{r}_3 0, 2; \chi). \quad (4.15d)$$

It is stressed that in the derivation of (4.15) no approximations other than those which can be justified in the bulk limit are introduced. The

terms on the right-hand side are, in general, describable in terms of  $g^{\langle}$ ,  $g^{\rangle}$ , and  $\chi$ . Since  $\chi$  are to be given as the initial condition, the set of the

four Eqs. (4.15) are *closed* equations with respect to  $g^<$  and  $g^>$  in contrast to the hierarchy equations such as (2.6) from which they are derived. The equations are highly nonlinear and non-Markovian.

However, fortunately for the purpose of formulating transport coefficients, these equations can be greatly simplified without the loss of rigor, which will be discussed in the forthcoming papers.

\*Research sponsored in part by the National Science Foundation Grant No. GP9040.

<sup>1</sup>N. Bogoliubov, *Problems of a Dynamical Theory in Statistical Physics* (OGIS, Moscow, 1946) [Trans: E. K. Gora, *Studies in Statistical Mechanics*, edited by J. De Boer and G. E. Uhlenbeck (North-Holland, Amsterdam, 1962), Vol. 1, p. 1]; M. Born and H. S. Green, *General Kinetic Theory of Fluids* (Cambridge U.P., London, 1949); J. G. Kirkwood, *J. Chem. Phys.* **14**, 180 (1946); **15**, 72

(1947); J. Yvon, *La Theorie Statistique des Fluids et l'Equation d'Etat* (Hermann, Paris, 1935).

<sup>2</sup>S. Fujita, *J. Phys. Soc. Japan* **26**, 505 (1969).

<sup>3</sup>S. Fujita, *Introduction to Non-Equilibrium Quantum Statistical Mechanics* (Saunders, Philadelphia, 1966).

<sup>4</sup>L. P. Kadanoff and G. Baym, *Quantum Statistical Mechanics* (Benjamin, New York, 1963).

<sup>5</sup>S. Fujita, *J. Phys. Soc. Japan* **27**, 1096 (1969).

<sup>6</sup>G. C. Wick, *Phys. Rev.* **80**, 268 (1950).

## Forward-Scattering Amplitudes and Fermi-Liquid Factors in Dilute Solutions of He<sup>4</sup> in Liquid He<sup>3</sup>

W. F. Saam

*Department of Physics, The Ohio State University, Columbus, Ohio 43210*

(Received 29 March 1971)

A derivation of exact expressions, given in terms of thermodynamic quantities, for the *s*-wave parts of the He<sup>3</sup>-He<sup>4</sup> and He<sup>4</sup>-He<sup>4</sup> quasiparticle forward-scattering amplitudes in very dilute solutions of He<sup>4</sup> in liquid He<sup>3</sup> is given. The result for the *p*-wave part of the He<sup>3</sup>-He<sup>4</sup> amplitude is related to the He<sup>4</sup> quasiparticle effective mass. The associated Fermi-liquid parameters are also derived.

### I. INTRODUCTION

In this paper we use a Green's-function formalism to derive exact equations for the He<sup>3</sup>-He<sup>4</sup> and He<sup>4</sup>-He<sup>4</sup> quasiparticle forward-scattering amplitudes in dilute solutions of He<sup>4</sup> in liquid He<sup>3</sup>. The *s*-wave parts of the He<sup>3</sup>-He<sup>4</sup> and He<sup>4</sup>-He<sup>4</sup> amplitudes are explicitly evaluated in terms of the thermodynamic quantities, and the *p*-wave part of the He<sup>3</sup>-He<sup>4</sup> amplitude is related to the He<sup>4</sup> quasiparticle effective mass. Only the cases of one and two He<sup>4</sup> atoms in liquid He<sup>3</sup> at  $T=0$  are considered. However, the results should be useful at all temperatures and He<sup>4</sup> concentrations where a quasiparticle picture is valid (i. e., for  $T \leq 0.1$  K in the one phase region on the He<sup>3</sup> rich side of the phase-separation curve). Qualitative arguments leading to many of the results herein have been presented elsewhere.<sup>1</sup> The present work thus provides a quantitative justification of these results within the limits of the quasiparticle description.

The two major results of this work are those for the *s*-wave parts of the He<sup>4</sup>-He<sup>3</sup> and He<sup>4</sup>-He<sup>4</sup> quasiparticle forward-scattering amplitudes ( $a_{43}^0$  and  $a_{44}^0$ , respectively) for He<sup>3</sup> quasiparticles on the Fermi surface and He<sup>4</sup> quasiparticles of very small momenta. We find (see also Ref. 1)

$$a_{43}^0 = (1 + \alpha)/\nu(0), \quad (1)$$

$$a_{44}^0 = \left( \frac{\partial \mu_4}{\partial n_4} \right)_{\mu_3}. \quad (2)$$

Here  $\alpha$  is the fractional excess volume occupied by a He<sup>4</sup> atom in liquid He<sup>3</sup>, and  $\nu(0)$  is the density of He<sup>3</sup> quasiparticle states at the Fermi surface.  $\mu_3$  and  $\mu_4$  are the He<sup>3</sup> and He<sup>4</sup> chemical potentials, and  $n_4$  is the He<sup>4</sup> number density. Using the result  $\alpha \approx 0.32$ ,<sup>2</sup> we obtain  $a_{43}^0 \approx 0.68/\nu(0)$ . The analogous quantities for parallel and antiparallel spin-quasiparticle scattering in pure He<sup>3</sup> are,<sup>3</sup> respectively,  $a_0^{\uparrow} = 2.9/\nu(0)$  and  $a_0^{\downarrow} = -1.1/\nu(0)$ . It follows then that the temperature range over which a quasiparticle picture for He<sup>4</sup>'s in He<sup>3</sup> may be expected to be valid is the same as that for He<sup>3</sup>'s, namely,  $T \leq 0.1$  K.  $a_{44}^0$  has been evaluated<sup>1</sup> using a rather plausible assumption concerning the nature of the phase-separation curve as the He<sup>4</sup> number concentration  $x$  and  $T$  approach zero. The result is

$$a_{44}^0 = 0. \quad (3)$$

It follows from (3) that the phase separation at small  $x$  is closely related to that in a noninteracting Bose gas.

Section II is devoted to a derivation of the exact